Journal of Ethnopharmacology 243 (2019) 112093

Contents lists available at ScienceDirect

Journal of Ethnopharmacology

journal homepage: www.elsevier.com/locate/jethpharm

Total ginsenosides extract induce autophagic cell death in NSCLC cells through activation of endoplasmic reticulum stress

Min Zhao[a,b,1], Qiufang Chen[c,1], Wanfeng Xu[a], Hong Wang[a], Yuan Che[a], Mengqiu Wu[a], Lin Wang[a], Cao Lijuan[a,*], Haiping Hao[a,**]

[a] State Key Laboratory of Natural Medicines, Key Lab of Drug Metabolism and Pharmacokinetics, China Pharmaceutical University, Nanjing, China
[b] Department of Pharmacy, The First Affiliated Hospital of Xiamen University, Xiamen, China
[c] Science and Education Division, Women and Children's Hospital, School of Medicine, Xiamen University, Xiamen, China

ARTICLE INFO

Keywords:
Total ginsenoside extract
Autophagy
Endoplasmic reticulum stress
Non-small cell lung cancer

ABSTRACT

Ethnopharmacological relevance: Ginseng (*Panax ginseng* C. A. Mey) has been widely used in Asian countries for thousands of years. It has auxiliary anticancer efficacy and its derived preparations (e.g. Shenmai injection) are prescribed for cancer patients as Traditional Chinese Medicines clinically in China.

Aim of the study: The involved adjuvant anticancer mechanisms of ginseng are still unknown. The present study evaluated the anti-cancer effect of total ginsenosides extract (TGS) and determined the anticancer mechanisms of TGS-induced cell death in human non-small cell lung cancer (NSCLC) cells.

Materials and methods: The anti-cancer effect of TGS was evaluated in NSCLC by cell proliferation assay. The autophagy flux induction of TGS were tested and validated by Western blot, immunofluorescence and transmission electron microscope. The mechanisms of TGS in inducing autophagic cell death were validated by Western blot, gene knockdown and quantitative real time PCR assay.

Results: We found TGS could induce cell death in concentration and time dependent manners, and the cell morphology of NSCLC changed from cobblestone shape to elongated spindle shape after treated with TGS. In the study of cell autophagy, we confirm that TGS could upregulate autophagy flux and induce autophagic cell death through activation endoplasmic reticulum stress. Further investigations demonstrated this process was mediated by the ATF4-CHOP-AKT1-mTOR axis in NSCLC cells.

Conclusion: Our findings suggested that TGS could induce autophagic cell death in NSCLC cells through activation of endoplasmic reticulum stress, disclosing another characteristic of TGS-induced cell death and a novel mechanism of TGS and its derived preparations in clinical treatment of cancer patients.

1. Introduction

Lung cancer is the leading cause of cancer death all over the world, and has surpassed breast cancer among females in more developed countries (Torre et al., 2016). Age-standardised 5-year net survival was in the range 10–20% in most countries (Desantis et al., 2014; Allemani et al., 2018). Non-small cell lung cancer (NSCLC) is the most common type of lung cancer and remains as a serious public health concern (Allemani et al., 2018).

Endoplasmic reticulum stress (ER stress) is a cellular response to protein misfolding, which has profound effect on cancer cell survival and death (Clarke et al., 2014). ER stress is involved in many diseases, such as central nervous system diseases, inflammation and cancer (Zhang et al., 2015; Cao et al., 2016; Wang et al., 2014). Unfolded

Abbreviations: 3-MA, 3-methyladenine; CCK-8, Cell Counting kit 8; CQ, chloroquine; FBS, fetal bovine serum; GAPDH, gluceraldelyde-3-phosphate dehydrogenase; MDC, monodansylcadaverine; NSCLC, non-small cell lung carcinoma; PBS, phosphate buffered saline; PBST, PBS containing 0.1% Tween-20; PMSF, Phenylmethanesulfonyl fluoride; qRT-PCR, quantitative real-time polymerase chain reaction; Rapa, rapamycin; siRNA, small interfering RNA; TBST, Tris-buffered saline containing 0.1% Tween-20; TGS, Total Ginsenosides extract; TUNEL, TdT-mediated dUTP Nick-End Labeling; WOM, wortmannin

* Corresponding author. China Pharmaceutical University, No.639 Longmian Avenue, Jiangning District, Nanjing, Jiangsu, 211198, China
** Corresponding author. China Pharmaceutical University, No.639 Longmian Avenue, Jiangning District, Nanjing, Jiangsu, 211198, China
E-mail addresses: zhaomincpupk@163.com (M. Zhao), chairxie@163.com (Q. Chen), 15251768808@163.com (W. Xu), wanghong991@163.com (H. Wang), cheyuancpu@163.com (Y. Che), mengqiuwu@126.com (M. Wu), lwang@sinnyt.ac.cn (L. Wang), caolijuan0702@cpu.edu.cn (C. Lijuan), hhp_770505@hotmail.com (H. Hao).
[1] These authors contributed equally to this work.

https://doi.org/10.1016/j.jep.2019.112093
Received 8 May 2019; Received in revised form 14 July 2019; Accepted 14 July 2019
Available online 17 July 2019
0378-8741/

protein response is activated during ER stress, and its markers including ATF-6, XBP-1 and ATF-4 along with BIP and CHOP (Khan et al., 2015). Autophagy is an evolutionarily conserved membrane-trafficking process that operates at basal levels under normal conditions as a means of degrading cytosolic proteins and organelles. In response to nutrient deprivation or trophic factor withdrawal, autophagy acts as a self-limited survival mechanism (Kimmelman and White, 2017). However, autophagosome accumulation is frequently observed within cells undergoing programmed cell death suggesting that autophagy may promote cell death, which was called Type II cell death (Silke and Meier, 2013). Therefore, autophagy regulates cell fate differently under different circumstances. ER stress is a potent trigger for autophagy, the relationship between ER stress and autophagy is intertwined and has been reviewed (Yorimitsu et al., 2006; Lee et al., 2015).

Many natural products have anti-cancer activity (Siveen et al., 2017; Taylor and Jabbarzadeh, 2017), however, the mechanisms are mostly unclear. Ginseng (*Panax ginseng* C. A. Mey)has been widely used in Asian countries for thousands of years and was prescribed as a dietary supplement for cancer patients in China (Jia and Zhao, 2009). The effective components of ginseng are multiple ginsenosides, including more than 100 kinds of protopanaxadiol (PPD)- and protopanaxatriol (PPT)-type ginsenosides (Christensen, 2009). The pharmacological activities of these ginsenosides have been identified in many articles (Murthy et al., 2018; Majeed et al., 2018). The effect of ginsenosides on autophagy in cancer differ from each other, some of them play a positive regulatory role, some negative, and act on different pathways (Kim et al., 2013; Ko et al., 2009). Ginseng and Shenmai injection (a Traditional Chinese Medicine preparation containing ginseng) are prescribed as herbal medicines for cancer patients in China. However, the effect of TGS on autophagy and its adjuvant anti-cancer mechanisms are still unclear.

In the present research, we studied the cytotoxicity of TGS on NSCLC cell and found that TGS could induce cell death in concentration and time dependent manners. Further investigations demonstrated that TGS induced autophagic cell death through activation of endoplasmic reticulum stress and mediated autophagy via the ATF4-CHOP-AKT1-mTOR axis, disclosing the characteristics of TGS induced cell death and a novel anti-cancer mechanism of TGS and its derived preparations in clinical.

2. Materials and methods

2.1. Reagents and cell culture

Total ginsenosides extract and ginsenosides monomers (purity 98%) were purchased from the College of Chemistry in Jilin University (Changchun, China). The contents of Total ginsenosides extract (Rb1 11.2%, Rb2 11.1%, Rc 10.5%, Rd7.7%, Re 8.9%, Rf 0.9%, Rg1 3.3%, Rg2 1.4%, and Rh1 0.2%) were determined using a validated liquid chromatography-mass spectrometry method in our laboratory (Hao et al., 2010). TGS was dissolved in RPMI 1640 medium at a concentration of 100 mg/ml. DMSO (Cat.No.D4540), monodansylcadaverine (MDC,Cat.No.30432), wortmannin (WOM,-Cat.No.12–338), rapamycin (Rapa,Cat.No. 553210), 3-methyladenine (3-MA,Cat.No.M9281) and chloroquine (CQ,Cat.No.C6628) were purchased from Sigma Aldrich (St Louis, MO); Lipofectamine iMAX (Cat.No.13778075), ATG7 siRNA (Cat.No.HSS116182), ATG5 siRNA (Cat.No.HSS114103) and control siRNA (medium GC,Cat.No.12935300) were purchased from Invitrogen Trading Shanghai Co. (Shanghai, China). Cell Counting Kit 8 (CCK-8,Cat.-No.CK04-500T) was purchased from Dojindo (Kumamoto, Japan). RPMI 1640 medium (Cat.No.31800022) was from GIBCO (California, USA). RIPA lysis buffer (Cat.No.P0013B), Hoechst 33342 (Cat.No.C1022), Triton X-100 (Cat.No.ST795), BCA Protein Assay Kit (Cat.No.0012) and other reagents were from Beyotime Biotechnology (Shanghai, China).

Human non-small-cell lung cancer A549 and PC-9 cell lines were obtained from the American Type Culture Collection (ATCC) (Maryland, USA) and cultured in RPMI 1640 medium supplemented with 10% FBS, 100 U/ml penicillin and 100 μg/ml streptomycin at 37 °C with 5% CO_2.

2.2. Cell proliferation assay

A549 and PC-9 cells with 80% confluence in 96-well plates were treated with 0.1, 0.125, 0.2, 0.25, 0.375, 0.5, 0.625, 0.75, 1, 1.5 mg/ml TGS for 24 or 48 h, cell viability was measured after treatment using the CCK-8 assay according to the manufacturer's instructions. The absorbance at 450 nm was measured using a BioTek, Synegy H1 Hybrid Reader (Vermont, USA).

2.3. Cell morphological observation

A549 and PC-9 cells with 80% confluence in 6-well plates were treated with 0.25,0.5 and 1 mg/ml TGS for 24 h, cells were washed and observed in the brightfield of Leica DMI3000B fluorescence microscope (Bensheim, Germany).

2.4. Western blotting analysis

A549 cells were collected and lysed in ice-cold RIPA lysis buffer containing 2 mmol/L PMSF. The protein concentrations in cell lysates were quantified using BCA Protein Assay Kit. Cell lysates contained 60 μg of protein were subjected to SDS–PAGE using 8%–12% gradient polyacrylamide gels (Bis-Tris Midi Gel, Life Technologies, USA) and analyzed by immunoblotting with corresponding. The same blots were probed with GAPDH antibody to normalize protein load. Protein levels was quantified by densitometry using Image Lab software.

The primary antibodies anti-LC3B (Cat.No.2775), anti-ATF4 (Cat.No.11815), anti-CHOP (Cat.No.5554), anti-BIP (Cat.No.3177), anti-ATG7 (Cat.No.8558), anti-ATG5 (Cat.No.12994T), anti-phospho-p70 S6 kinase (Cat.No.9205) antibodies and horseradish peroxidase-conjugated goat anti-mouse/rabbit IgG secondary antibodies (Cat.No.7076/7074) were purchased from Cell Signaling Technology (Danvers, MA, USA), anti-p-AKT-1 antibody (Cat.No.ab66138) was purchased from Santa Cruz Biotechnology (Dallas, MA,USA) and anti-GAPDH antibody (Cat.No.AP0063) was purchased from Bioworld Technology (Nanjing, China).

2.5. Immunofluorescence

A549 cells were cultured in 0.17 mm glass-bottom dishes and incubated with agents for the indicated times, after which cells were fixed with 4% formaldehyde for 20 min at 4 °C, permeabilized with PBS/T (PBS containing 0.1% Tween-20) for 20 min at room temperature, blocked with 5% w/v BSA in PBS/T for 1 h at 37 °C and then incubated with primary antibodies overnight at 4 °C, after washed with PBS/T for 4 times, cells were incubated with fluorescent secondary antibody and Hoechst 33342 for 1 h in the dark, then cells were washes and observed with a Zeiss LSM 700 confocal fluorescence microscope (Oberkochen, Germany).

2.6. MDC staining

A549 cells were cultured in 12-well plates and treated with 200 nM rapamycin, 0.5 or 1 mg/ml TGS with or without 1 μM wortmannin or 5 mM 3-methyladenine for 6 h, then cells were stained with 50 μM MDC for 20 min at 37 °C, washed and observed with a Leica DMI3000B fluorescence microscope (Bensheim, Germany).

Table 1
The sequences of siRNA duplex for ATG7 siRNA and ATG5 siRNA.

Genes	sense strand	antisense strand
ATG5	5′-GCCGUCAUUGCUGCAAGCAAGAGAA-3′	5′-UUCUCUUGCUUGCAGCAAUGACGGC-3′
ATG7	5′-GGUUUGGACGAAUUCCAACUUGUUU-3′	5′-AAACAAGUUGGAAUUCGUCCAAACC-3′

Table 2
Primer sequences for quantitative RT-PCR Assay.

Genes	forward 5′-3′	reverse 5′-3′
GAPDH	CCAGGGCTGCTTTTAACTC	GCTCCCCCCTGCAAATGA
ATF4	GAAGGTCATCTGGCATGGTT	AGTCCCTCCAACAACAGCAA
CHOP	ACCAAGGGAGAACCAGGAAACG	TCACCATTCGGTCAATCAGAGC
BIP	GCTATTGCTTATGGCCTGGA	CGCTGGTCAAAGTCTTCTCC

2.7. Transmission electron microscope observation of subcellular structures

A549 cells were treated with 0.5 or 1 mg/ml TGS with or without 1 μM wortmannin or 5 mM 3-methyladenine for 6 h, after which cells were fixed with 2.5% glutaraldehyde and 1% osmium tetroxide successively, and dehydrated with a range of concentrations of acetone, after penetrated and embedded, cells were sliced on ultramicrotome and electronic dyed with sodium acetate and lead citrate, finally, slices were observed with JEM-1010 transmission electron microscope (JEOL, Japan).

2.8. Gene knockdown

All transfections were performed using Lipofectamine iMAX according to the manufacturer's instructions. Cells were transfected with ATG7 siRNA, ATG5 siRNA or negative control (medium GC) at concentrations of 15 and 30 nM (ATG7 siRNA) or 20 nM (ATG5 siRNA). The sequences of siRNA duplex for ATG7 siRNA and ATG5 siRNA are shown in Table 1.

2.9. Quantitative real time PCR assay

Total RNA extraction was performed using RNAiso Plus reagent (TaKaRa Biotechnology Co., Ltd, Dalian, China) according to the manufacturer's protocol. The concentration of RNA was determined by measuring the absorbance at 260 and 320 nm. Complementary DNA was generated from 500 ng total RNA using Super Script II Reverse Transcriptase (Life Technology). Quantitative real time PCR analysis was carried out using SYBR green PCR master mix (TaKaRa Biotechnology Co., Ltd.) in a reaction volume of 15 μl. Real-time PCR was performed by using a Bio-Rad C1000™ Thermal cycler RT-PCR system (Carlsbad, CA, USA). The annealing was performed at 60 °C for 30 s. Relative gene expression analysis was performed using the 2 ($^{-\Delta\Delta Ct}$) method with GAPDH as a housekeeping control. Each experiment was conducted in duplicates. The primer sequences are shown in Table 2. (forward 5′-3′, reverse 5′-3′).

2.10. Statistical analysis

Data were expressed as mean ± standard error of the mean (S.E.M.). Prism 6.0 statistical software was used for the analysis. The two-tailed Student *t*-test was used to reveal statistical significance. $P < 0.05$ was considered statistically significant.

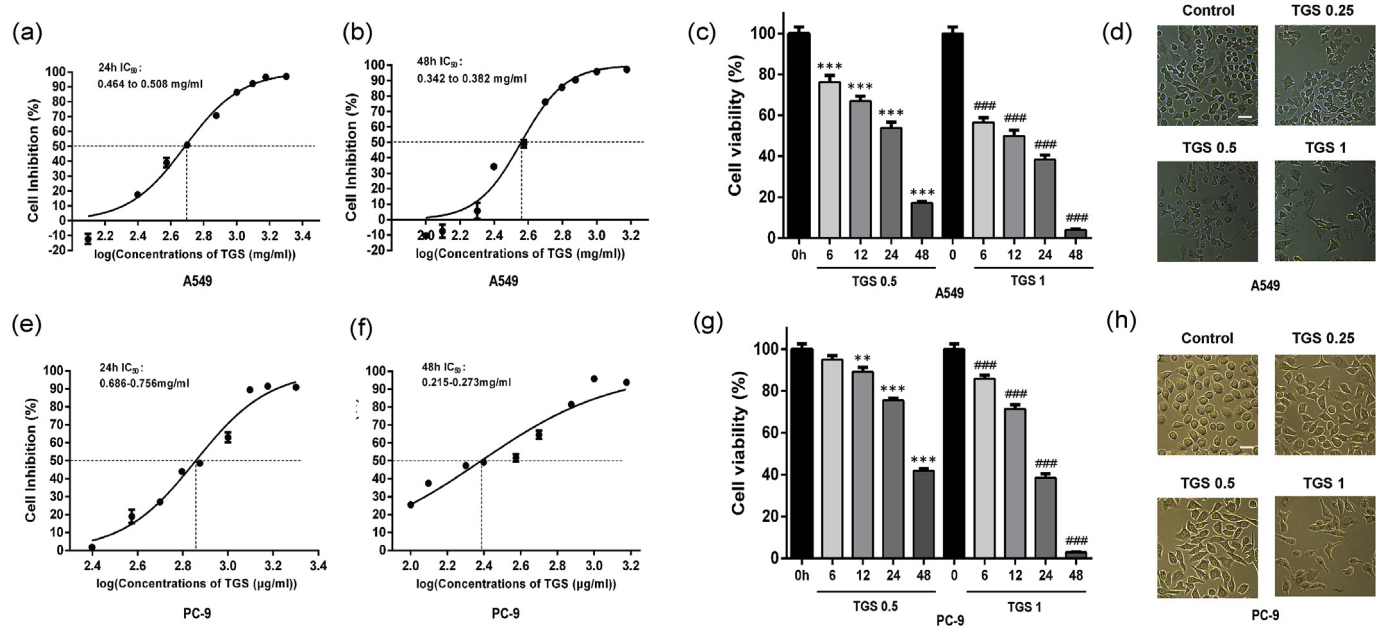

Fig. 1. TGS induces cell death in concentration and time dependent manners in NSCLC cells. (a)(b)(e)(f) Survival curve describing the viability of A549 cells (a)(b) or PC-9 cells (e)(f) treated with the indicated concentrations of TGS (mg/ml) for 24 or 48 h. The data was expressed as cell inhibition relative to untreated controls and represented the average value ± S.E.M. n = 3 for each group. (c)(g) Cell viability of A549 cells (c) or PC-9 cells (g) treated with the 0.5 or 1 mg/ml TGS for 24 or 48 h. The data was expressed as cell viability relative to untreated controls and represented the average value ± SEM. n = 3 for each group, $^{*}P < 0.05$, $^{**}P < 0.01$, $^{***}P < 0.001$ versus 0 h (TGS 0.5), $^{\#}P < 0.05$, $^{\#\#}P < 0.01$, $^{\#\#\#}P < 0.001$ versus 0 h (TGS1). (d)(h) Cell morphological observation after treated with 0.25,0.5,1 mg/ml TGS for 24 h, A549 cells (d), PC-9 cells (h). Scale bars, 20 μm.

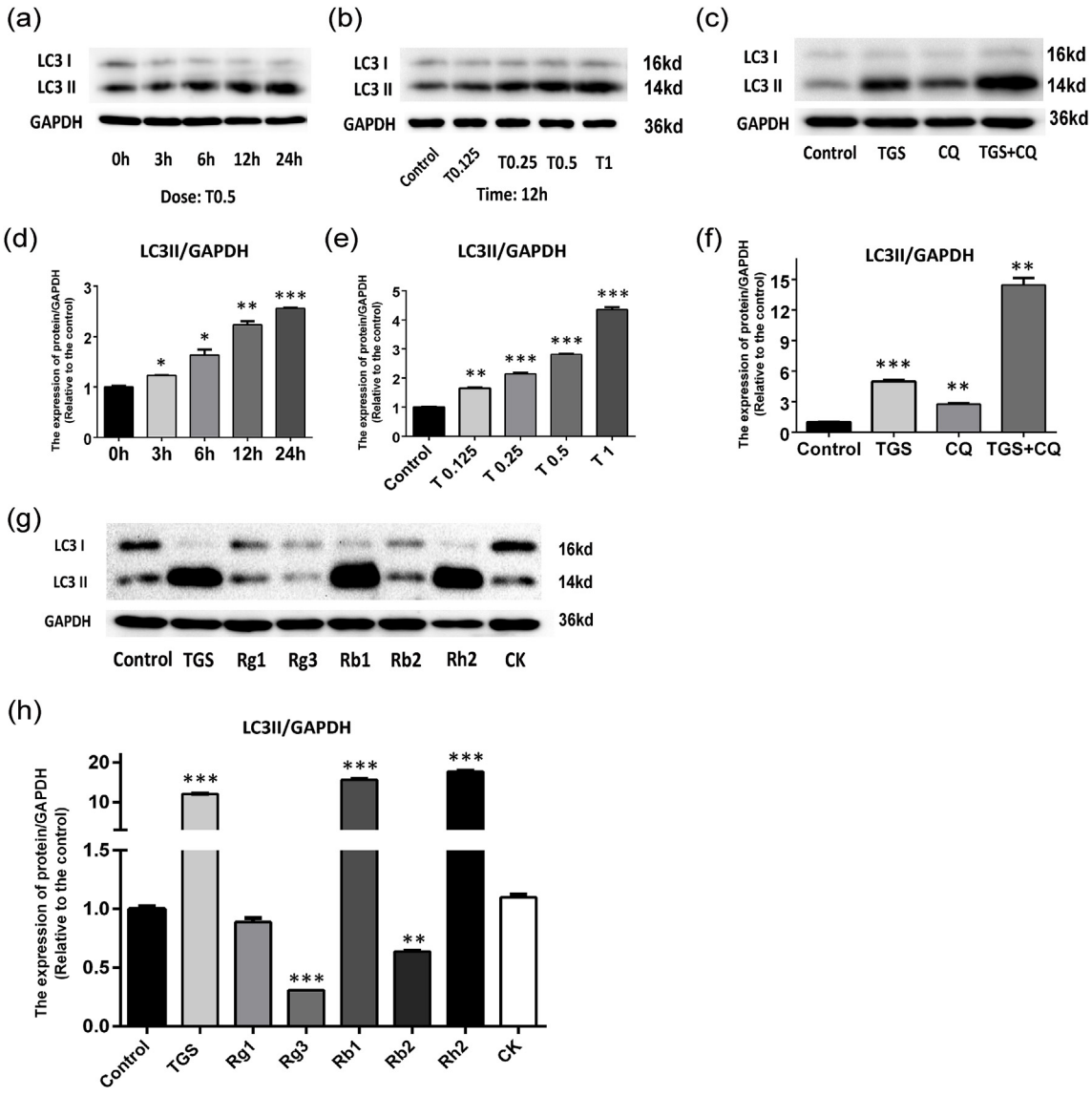

Fig. 2. TGS increases autophagy flux in a concentration and time dependent manner in NSCLC A549 cells. (a)(b) Immunoblot analysis with the LC3B antibody on cell lysates treated with 0.5 mg/ml TGS for 0, 3, 6, 12, 24 h (a) or a series concentrations of TGS (T0.125 represented 0.125 mg/ml TGS, and so on, the same below) for 12 h (b), GAPDH serves as a loading control. (c) LC3B turnover assay: A549 cells were treated with 0.5 mg/ml TGS (TGS) with or without 10 μM chloroquine (CQ) for 6 h, LC3B in cell lysates was detected with immunoblot, GAPDH serves as a loading control. (d)(e)(f) The semi-quantitative results of LC3II/GAPDH of (a)(b)(c) using the Volume Tool in Image lab software. (g) Effect of ginsenosides monomer on autophagy flux. A549 cells were treated with corresponding agents for 12 h (TGS: 0.5 mg/ml, Rg1:50 μM, Rg3:100 μM, Rb1:50 μM, Rb2:50 μM, Rh2:10 μM, CK:10 μM), total cellular were protein detected with LC3B antibody, GAPDH serves as a loading control. (h) The semi-quantitative results of LC3II/GAPDH of (g) using the Volume Tool in Image lab software. $^{*}P < 0.05$, $^{**}P < 0.01$, $^{***}P < 0.001$ versus 0 h or control.

3. Results

3.1. TGS induces cell death in concentration and time dependent manners in NSCLC cells

Firstly, we tested the cytotoxicity of TGS on NSCLC A549 and PC-9 cell lines, the results showed TGS induced cell death in concentration and time dependent manners (Fig. 1a, 1b, 1c, 1e, 1f & 1g). The IC_{50} of TGS in A549 cells were 0.464–0.508 mg/ml and 0.342–0.382 mg/ml for 24 h and 48 h respectively, the IC_{50} of TGS in PC-9 cells were 0.686–0.756 mg/ml and 0.215–0.273 mg/ml for 24 h and 48 h respectively. Cell morphological observation showed that A549 and PC-9 cells changed from cobblestone shape to mesenchymal-like and elongated spindle shape after treated with TGS (Fig. 1d & 1h), cell adhesion was reduced and exhibited an autophagic cell death-like morphology (Tsai Ch et al., 2017). These results reveal that TGS has obviously cytotoxicity in NSCLC cells and maybe a cell autophagy-induced effect.

3.2. TGS increases autophagy flux in a concentration and time dependent manner in NSCLC A549 cells

To test the effect of TGS on cell autophagy, we treated human NSCLC A549 cells with a series concentrations of TGS for different times and examined the level of MAP1LC3B-II (LC3 II) formation, a hallmark of autophagy (Mizushima et al., 2010). After treated with TGS, LC3 II levels increased in both concentration and time dependent manners (Fig. 2a&2b). To monitor the effect of TGS on autophagy flux, we conducted LC3 turnover assays by using chloroquine (CQ), a late stage autophagic inhibitor. The difference in LC3-II levels in the presence and absence of chloroquine is larger under TGS treatment (compare lanes 2 and 4, Fig. 2c), indicating that autophagy flux is increased during TGS treatment (Mizushima et al., 2010). The semi-quantitative results of

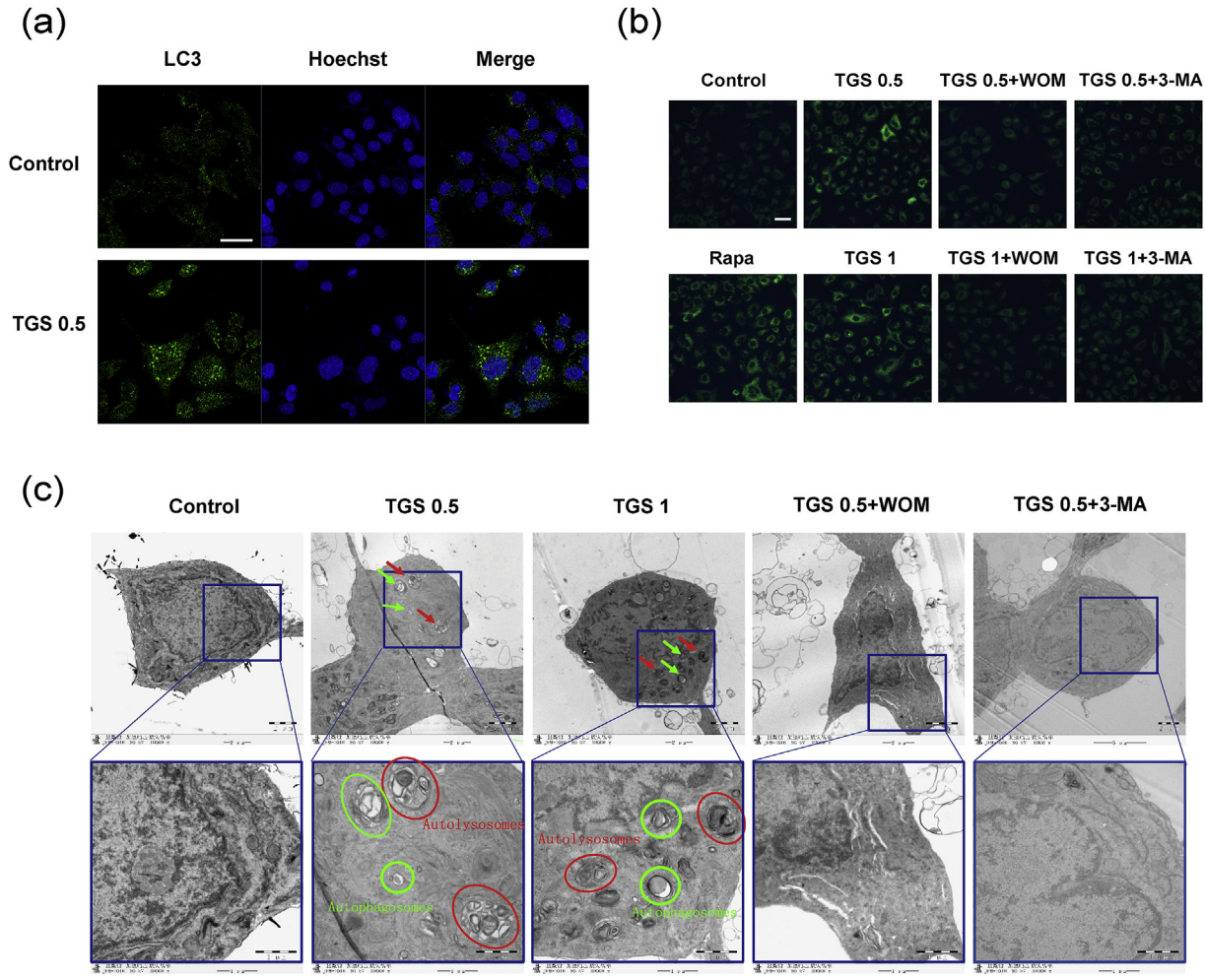

Fig. 3. Visual image confirmation of cell autophagy induction of TGS. (a) Immunofluorescence analysis of LC3 puncta formation in cells treated with 0.5 mg/ml TGS (TGS 0.5) for 6 h, Hoechst 33342 was used to stain the nuclei. Experiment was performed in triplicate and representative images were showed. Scale bars, 20 μm. (b) A549 cells were treated with 200 nM rapamycin (Rapa), 0.5,1 mg/ml TGS (TGS 0.5,1) with or without 1 μM wortmannin (WOM), 5 mM 3-methyladenine (3-MA) for 6 h, autophagosome formation was indicated by the green stains of MDC detected under 512 nm. Experiment was performed in triplicate and representative images were showed. Scale bars, 20 μm. (c) The transmission electron microscopy images of the A549 cells treated with 0.5, 1 mg/ml TGS (TGS 0.5, 1) with or without 1 μM wortmannin (WOM), 5 mM 3-methyladenine (3-MA) for 6 h, representative images were showed. Circles and arrows in green represented autophagosomes, and red ones indicated autolysosomes. Scale bars, 2 μm, insets 1 μm. . (For interpretation of the references to colour in this figure legend, the reader is referred to the Web version of this article.)

LC3II/GAPDH were showed as Fig. 2d, 2e, and 2f. The effects of ginsenoside monomers on autophagy showed that ginsenoside Rb1 and Rh2 mainly contributed to the autophagy induced effect of TGS (Fig. 2g & 2h). By immunofluorescence for LC3 staining, TGS was found to promote the formation of LC3 puncta (Fig. 3a). MDC staining demonstrated that TGS promoted the formation of autophagosome (Fig. 3b), which was further validated by transmission electron microscopy (Fig. 3c). Collectively, these results suggested that TGS increases autophagy flux in human NSCLC cells.

3.3. TGS induces autophagic cell death in NSCLC A549 cells

To determine whether TGS induced autophagic cell death, we co-treated A549 cells with TGS and autophagy inhibitors. We found that TGS-induced cell death was significantly blocked by autophagy inhibitors (Fig. 4a), suggesting an autophagy dependent manner of TGS-induced cell death. To further validate these results, we silenced ATG7 and ATG5 which are indispensable genes related to the initiation and development of autophagy in A549 cells with target si-RNA, the verification of silence efficiency were showed as Fig. 4b and d. We found a significant cell inhibition reverse effect of ATG7 and ATG5 knockdown compared with si-control (Fig. 4c & 4e). These data suggest that TGS induces autophagic cell death in NSCLC cells.

3.4. TGS induces autophagic cell death through activation of endoplasmic reticulum stress

To determine whether endoplasmic reticulum (ER) stress, a closely related signaling pathways involved in regulation of autophagy (Li et al., 2013), plays an important role in TGS-induced autophagy, we measured the mRNA and protein levels of ATF4, CHOP and BIP, which are typically regarded as hallmarks of ER stress response. The results showed that the mRNA and protein levels of these genes increase in both time and concentration dependent manners after treated with TGS (Fig. 5a, 5b, 5c, 5d, 5e, 5f, 5g & 5h), suggesting TGS activated ER stress in A549 cells. The semi-quantitative results of protein/GAPDH were showed as Fig. 5i–5j. On the other hand, we detected the levels of phospho-AKT1 (p-AKT1), phospho-p70 S6 kinase (a mTOR substrate) and ATG7 in human NSCLC cell lines A549. The results showed that TGS prevent the phosphorylation of AKT-1 and p70 S6 kinase, upregulated the levels of ATG7 in both time and concentration dependent manners (Fig. 5k& 5l), suggesting that autophagy was induced by TGS

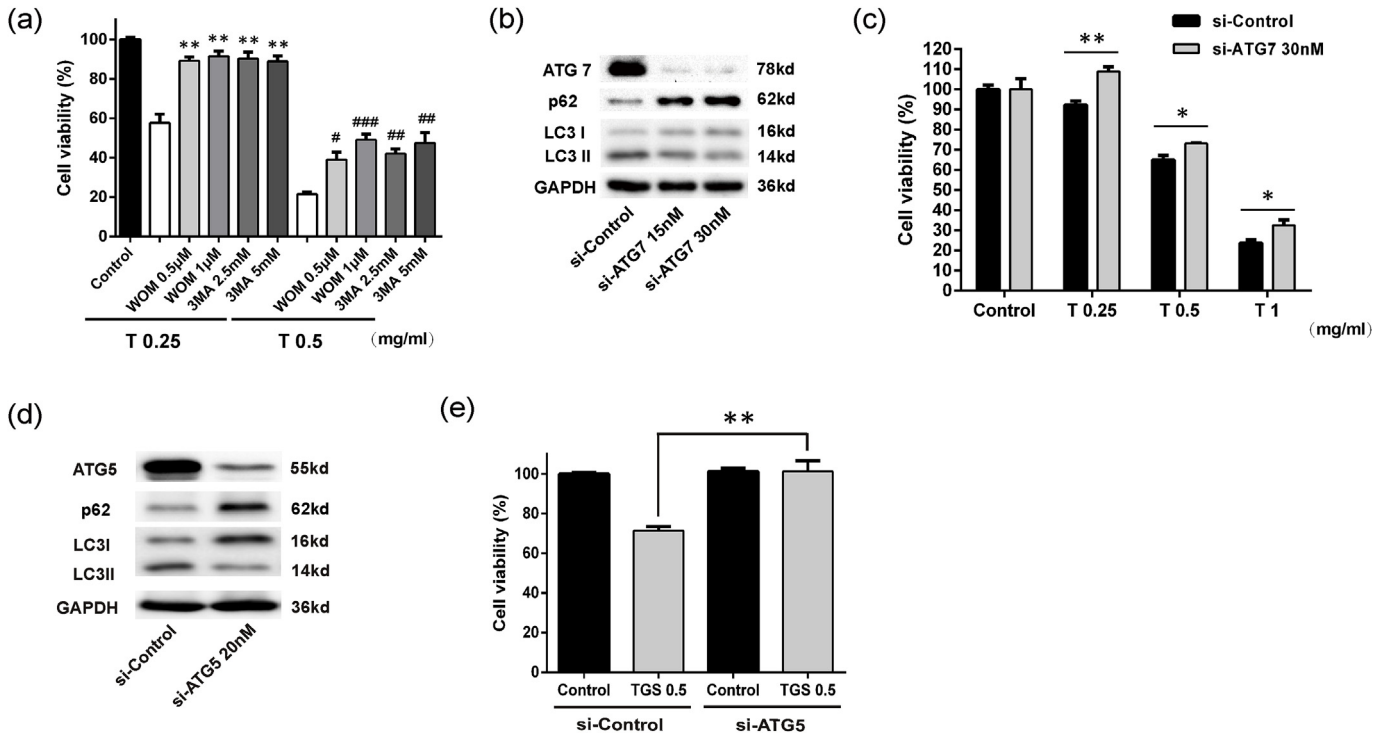

Fig. 4. TGS induces autophagic cell death in NSCLC A549 cells. (a) A549 cells were treated with 0.25,0.5 mg/ml TGS with or without 0.5,1 μM wortmannin (WOM), 2.5, 5 mM 3-methyladenine (3-MA) for 48 h, cell viability was detected with CCK-8, $^{*}P < 0.05$, $^{**}P < 0.01$, $^{***}P < 0.001$ versus T 0.25, $^{\#}P < 0.05$, $^{\#\#}P < 0.01$, $^{\#\#\#}P < 0.001$ versus T 0.5. (b)(d) Verification of ATG7 or ATG5 knockdown in A549 cells. (c)(e) Effect of TGS treatment (24 h) on cell viability transfected with control siRNAs (si-Control) or ATG 7- and ATG5-selective siRNA (si-ATG7 and si-ATG5), $^{*}P < 0.05$, $^{**}P < 0.01$ versus si-control.

via AKT1-mTOR inhibition in human NSCLC cells. The semi-quantitative results of protein/GAPDH were showed as Fig. 5m and n. Taken together, these data indicated that TGS induces autophagic cell death through activation of ER stress in human NSCLC cells.

4. Discussion

Autophagy is a metabolic process in which cell exogenous materials were degradated and recovered by lysosomes to achieve cell homeostasis. Basal and low physiological levels of autophagy is important for survival of cells under stress, however, a persistent or excessive autophagy could lead to cell death (Andon and Fadeel, 2013). Autophagic cell death is a selective and programmed cell death differ from cell apoptosis (Maiuri et al., 2007). This form of cell death usually referred to as caspase-independent cell death accompanied by autophagy and is dependent on multiple autophagy related genes (ATG) (Shen et al., 2012). The crosstalk between autophagy and apoptosis is controversial, most of scholars believe that autophagy is a self-protection mechanism of cells, which can prevent further apoptosis (Das et al., 2013; Avniel-Polak et al., 2015; Dodson et al., 2013), others hold the opinion that autophagy can promote apoptosis (Mattiolo et al., 2015; Petersen et al., 2014; Scott et al., 2007; Wang et al., 2010), more details can be found in this review (Maiuri et al., 2007). Many chemotherapy agents and natural products exert their anticancer effect via inducing autophagic cell death (Shingu et al., 2009; Xi et al., 2011; Kim et al., 2013).

Natural medicines are indispensable sources for the development of modern drugs, many natural products have anti-tumor effect, however, the targets and mechanism of which were unclear (Reddy et al., 2003; Hao et al., 2014). Ginseng is the most widely used traditional Chinese medicine in Asian countries. There are a lot of studies that investigate the regulation of ginsenosides on autophagy and apoptosis. Most of these studies are ginsenosides monomers and rarely with total ginsenoside as the object of study while ginseng and its derived preparations are prescribed as whole compound preparations for patients in clinical. Ginseng's auxiliary anticancer mechanism has not been fully elucidated.

In the present study, we first investigated the cytotoxicity of TGS on NSCLC cells, and found TGS induced cell death in time and concentration dependent manners. The sensitivity of PC-9 cell line to TGS changed more with time than that of A549 cell line. A549 is an EGFR wild-type cell line, while PC-9 is an EGFR-mutant (with E746-A750 deleted). The different expressions and mutations of EGFR in two cell lines may be the reason for the above results, but we have not verified it yet. We will continue to focus on and study these interesting findings. In our previous study, 40 mg/kg TGS once a day for two weeks significantly enhanced the anti-tumor effect of mitomycin C *in vivo*, but did not cause visible damage to normal tissues, nor did the mice lose weight (Zhao et al., 2017). In our another study about TGS alleviating ROS-induced cardiomyocyte injury, the treatment of rat cardiomyocyte H9c2 with 125 μg/ml (low concentration group in this study) TGS for 24 h did not show any cell damage, but significantly antagonized ROS-induced cardiomyocyte injury (the data has not been published, so it is not shown). Based on the above studies, we believe that TGS has selective toxicity to cancer cells and cause little damage to normal tissue, so it has therapeutic value. There are many reports focused on the cancer cell apoptosis induction of ginsenosides (Wong et al., 2010; Chen et al., 2016), however, NSCLC cells appeared an autophagic cell death-like morphology after treated with TGS in our study, which lead us to investigate its autophagy induction rather than apoptosis. Our previous study have shown that TGS has less inductive effect on apoptotic related genes in NSCLC cells, including capase family and proapoptosis genes in Bcl-2 family (Zhao et al., 2017). The results of immunoblotting and immunofluorescence demonstrated that the level of LC3 II, a specific marker of autophagy, was increased after treated with TGS, suggesting the autophagy flux induction of TGS. MDC staining and transmission electron microscope observation further validated that TGS could promote the formation of autophagosome and autolysosome in NSCLC cells. The effects of ginsenoside monomers on autophagy showed that ginsenoside Rb1 and Rh2 mainly contributed to the

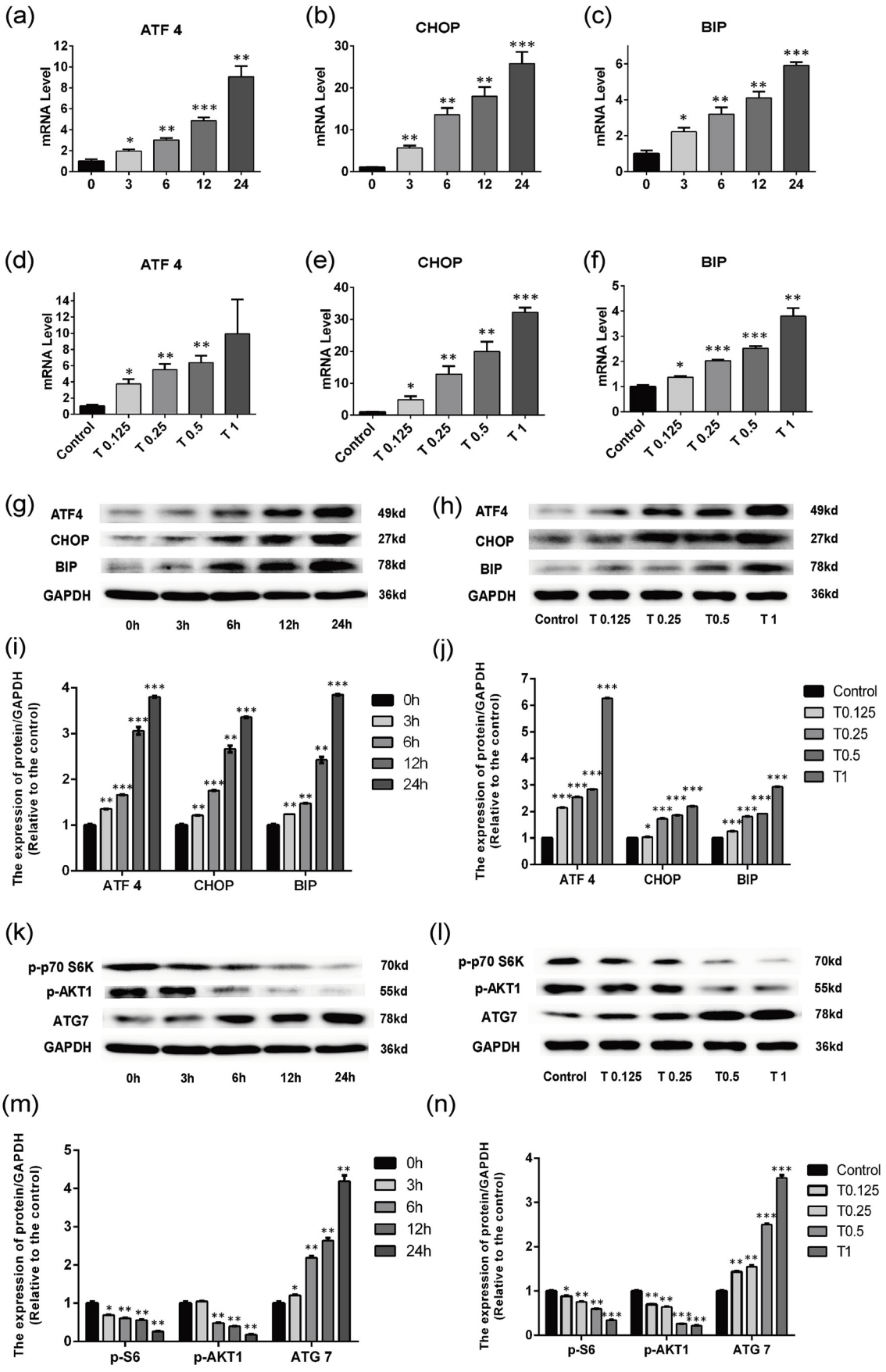

(caption on next page)

Fig. 5. TGS induces autophagic cell death through activation of endoplasmic reticulum stress. (a)(b)(c)(d)(e)(f) Quantitative RT-PCR analysis of mRNA levels of ATF4,CHOP, BIP in A549 cells treated with 0.5 mg/ml TGS for 0, 3,6,12,24 h (a,b,c) or a series concentrations of TGS for 12 h (d,e,f, T0.25 represented 0.25 ml/ml TGS, and so on), mRNA level were relative to 0 h or control, GAPDH serves as a housekeeping control. $*P < 0.05$, $**P < 0.01$, $***P < 0.001$ versus 0 h or control. (g)(h)(k)(l) Immunoblot analysis with the indicated antibodies on cell lysates treated with a series concentrations of TGS for 12 h (g,k) or 0.5 mg/ml TGS for 0,3,6,12,24 h (h,l), GAPDH serves as a loading control. (i)(j)(m)(n) The semi-quantitative results of protein/GAPDH of (g)(h)(k)(l) using the Volume Tool in Image lab software. $*P < 0.05$, $**P < 0.01$, $***P < 0.001$ versus 0 h or control.

autophagy induced effect of TGS, these results have some differences with other publications maybe due to the different experimental conditions and cell strains (Kim et al., 2013; Luo et al., 2014). Prophase inhibitors of autophagy significantly partly reversed the cytotoxicity of TGS, suggesting the autophagy dependent manner of TGS-induced cell death. The knockdown assays of ATG7 and ATG5 further validated the above view. We analyzed each pair of LC3-I and II on the same PAGE, the contrast of LC3 image provided in each figure may be a little different and we tried to provide images with grey background. The slightly up-regulation of LC3-II expression in si-control groups in Fig. 4 maybe related to the experimental conditions, gene knockdown assay have certain damage on cells, which may lead to stress autophagy. In the following studies, we found that TGS could induce endoplasmic reticulum stress, an important autophagy initiated fator. The results of the investigation of this pathway showed that TGS induced autophagy via the ATF4-CHOP-AKT1-mTOR axis, which has a similar autophagy-induced property with salinomycin, a promising anti-cancer compound (Li et al., 2013; Gupta et al., 2009).

5. Conclusions

In summary, we conclude that TGS induce autophagic cell death in NSCLC cells through activation of endoplasmic reticulum stress. Our present study disclosed another characteristic of TGS-induced cell death and a novel anti-cancer mechanism of TGS and its derived preparations in clinical, suggesting TGS and its derived preparations could be promising therapies for cancer patients.

Conflicts of interest

The authors declare that there are no conflict of interests.

Author contributions

Min Zhao, Lijuan Cao and Haiping Hao conceived the study. Min Zhao and Qiufang Chen initiated and designed and performed the experiments, analyzed and interpreted data, performed statistical analysis, wrote the initial manuscript. Wanfeng Xu, Yuan Che, Hong Wang, Mengqiu Wu and Lin Wang assisted to perform the experiments and analyze and interpret data, perform statistical analysis. Lijuan Cao assisted to review the manuscript. Lijuan Cao and Haiping Hao funded the experiment, reviewed the manuscript, and approved the final version of the manuscript.

Acknowledgement and Funding

This study was financially supported by the National Natural Science Foundation of China (grants No.91429308, 8153000588 and 81603193) and the project for Major New Drugs Innovation and Development (grant 2015ZX09501010).

Appendix A. Supplementary data

Supplementary data to this article can be found online at https://doi.org/10.1016/j.jep.2019.112093.

References

Allemani, C., Matsuda, T., Di Carlo, V., Harewood, R., Matz, M., Niksic, M., Bonaventure, A., Valkov, M., Johnson, C.J., Esteve, J., Ogunbiyi, O.J., Azevedo, E.S.G., Chen, W.Q., Eser, S., Engholm, G., Stiller, C.A., Monnereau, A., Woods, R.R., Visser, O., Lim, G.H., Aitken, J., Weir, H.K., Coleman, M.P., 2018. Global surveillance of trends in cancer survival 2000-14 (CONCORD-3): analysis of individual records for 37 513 025 patients diagnosed with one of 18 cancers from 322 population-based registries in 71 countries. Lancet 391, 1023–1075.

Andon, F.T., Fadeel, B., 2013. Programmed cell death: molecular mechanisms and implications for safety assessment of nanomaterials. Acc. Chem. Res. 46, 733–742.

Avniel-Polak, S., Leibowitz, G., Riahi, Y., Glaser, B., Gross, D.J., Grozinsky-Glasberg, S., 2015. Abrogation of autophagy by chloroquine alone or in combination with mTOR inhibitors induces apoptosis in neuroendocrine tumor cells. Neuroendocrinology 103, 724–737.

Cao, S.S., Luo, K.L., Shi, L., 2016. Endoplasmic reticulum stress interacts with inflammation in human diseases. J. Cell. Physiol. 231, 288–294.

Chen, L., Meng, Y., Sun, Q., Zhang, Z., Guo, X., Sheng, X., Tai, G., Cheng, H., Zhou, Y., 2016. Ginsenoside compound K sensitizes human colon cancer cells to TRAIL-induced apoptosis via autophagy-dependent and -independent DR5 upregulation. Cell Death Dis. 7, e2334.

Christensen, L.P., 2009. Ginsenosides chemistry, biosynthesis, analysis, and potential health effects. Adv. Food Nutr. Res. 55, 1–99.

Clarke, H.J., Chambers, J.E., Liniker, E., Marciniak, S.J., 2014. Endoplasmic reticulum stress in malignancy. Cancer Cell 25, 563–573.

Das, A., Pushparaj, C., Herreros, J., Nager, M., Vilella, R., Portero, M., Pamplona, R., Matias-Guiu, X., Marti, R.M., Canti, C., 2013. T-type calcium channel blockers inhibit autophagy and promote apoptosis of malignant melanoma cells. Pigment Cell Melanoma. Res. 26, 874–885.

Desantis, C.E., Lin, C.C., Mariotto, A.B., Siegel, R.L., Stein, K.D., Kramer, J.L., Alteri, R., Robbins, A.S., Jemal, A., 2014. Cancer treatment and survivorship statistics, 2014. CA Cancer J Clin 64, 252–271.

Dodson, M., Liang, Q., Johnson, M.S., Redmann, M., Fineberg, N., Darley-Usmar, V.M., Zhang, J., 2013. Inhibition of glycolysis attenuates 4-hydroxynonenal-dependent autophagy and exacerbates apoptosis in differentiated SH-SY5Y neuroblastoma cells. Autophagy 9, 1996–2008.

Gupta, P.B., Onder, T.T., Jiang, G., Tao, K., Kuperwasser, C., Weinberg, R.A., Lander, E.S., 2009. Identification of selective inhibitors of cancer stem cells by high-throughput screening. Cell 138, 645–659.

Hao, H., Lai, L., Zheng, C., Wang, Q., Yu, G., Zhou, X., Wu, L., Gong, P., Wang, G., 2010. Microsomal cytochrome p450-mediated metabolism of protopanaxatriol ginsenosides: metabolite profile, reaction phenotyping, and structure-metabolism relationship. Drug Metab. Dispos. 38, 1731–1739.

Hao, H., Zheng, X., Wang, G., 2014. Insights into drug discovery from natural medicines using reverse pharmacokinetics. Trends Pharmacol. Sci. 35, 168–177.

Jia, L., Zhao, Y., 2009. Current evaluation of the millennium phytomedicine–ginseng (I): etymology, pharmacognosy, phytochemistry, market and regulations. Curr. Med. Chem. 16, 2475–2484.

Khan, M.M., Yang, W.L., Wang, P., 2015. Endoplasmic reticulum stress in sepsis. Shock 44, 294–304.

Kim, A.D., Kang, K.A., Kim, H.S., Kim, D.H., Choi, Y.H., Lee, S.J., Kim, H.S., Hyun, J.W., 2013. A ginseng metabolite, compound K, induces autophagy and apoptosis via generation of reactive oxygen species and activation of JNK in human colon cancer cells. Cell Death Dis. 4, e750.

Kimmelman, A.C., White, E., 2017. Autophagy and tumor metabolism. Cell Metabol. 25, 1037–1043.

Ko, H., Kim, Y.J., Park, J.S., Park, J.H., Yang, H.O., 2009. Autophagy inhibition enhances apoptosis induced by ginsenoside Rk1 in hepatocellular carcinoma cells. Biosci. Biotechnol. Biochem. 73, 2183–2189.

Lee, W.S., Yoo, W.H., Chae, H.J., 2015. ER stress and autophagy. Curr. Mol. Med. 15, 735–745.

Li, T., Su, L., Zhong, N., Hao, X., Zhong, D., Singhal, S., Liu, X., 2013. Salinomycin induces cell death with autophagy through activation of endoplasmic reticulum stress in human cancer cells. Autophagy 9, 1057–1068.

Luo, T., Liu, G., Ma, H., Lu, B., Xu, H., Wang, Y., Wu, J., Ge, P., Liang, J., 2014. Inhibition of autophagy via activation of PI3K/Akt pathway contributes to the protection of ginsenoside Rb1 against neuronal death caused by ischemic insults. Int. J. Mol. Sci. 15, 15426–15442.

Maiuri, M.C., Zalckvar, E., Kimchi, A., Kroemer, G., 2007. Self-eating and self-killing: crosstalk between autophagy and apoptosis. Nat. Rev. Mol. Cell Biol. 8, 741–752.

Majeed, F., Malik, F.Z., Ahmed, Z., Afreen, A., Afzal, M.N., Khalid, N., 2018. Ginseng phytochemicals as therapeutics in oncology: recent perspectives. Biomed. Pharmacother. = Biomed. Pharmacother. 100, 52–63.

Mattiolo, P., Yuste, V.J., Boix, J., Ribas, J., 2015. Autophagy exacerbates caspase-dependent apoptotic cell death after short times of starvation. Biochem. Pharmacol. 98, 573–586.

Mizushima, N., Yoshimori, T., Levine, B., 2010. Methods in mammalian autophagy research. Cell 140, 313–326.
Murthy, H.N., Dandin, V.S., Park, S.Y., Paek, K.Y., 2018. Quality, safety and efficacy profiling of ginseng adventitious roots produced in vitro. Appl. Microbiol. Biotechnol. 102, 7309–7317.
Petersen, M., Hofius, D., Andersen, S.U., 2014. Signaling unmasked: autophagy and catalase promote programmed cell death. Autophagy 10, 520–521.
Reddy, L., Odhav, B., Bhoola, K.D., 2003. Natural products for cancer prevention: a global perspective. Pharmacol. Ther. 99, 1–13.
Scott, R.C., Juhasz, G., Neufeld, T.P., 2007. Direct induction of autophagy by Atg1 inhibits cell growth and induces apoptotic cell death. Curr. Biol. 17, 1–11.
Shen, S., Kepp, O., Kroemer, G., 2012. The end of autophagic cell death? Autophagy 8, 1–3.
Shingu, T., Fujiwara, K., Bogler, O., Akiyama, Y., Moritake, K., Shinojima, N., Tamada, Y., Yokoyama, T., Kondo, S., 2009. Inhibition of autophagy at a late stage enhances imatinib-induced cytotoxicity in human malignant glioma cells. Int. J. Cancer 124, 1060–1071.
Silke, J., Meier, P., 2013. Inhibitor of apoptosis (IAP) proteins-modulators of cell death and inflammation. Cold Spring Harb Perspect. Biol. 5, a008730.
Siveen, K.S., Uddin, S., Mohammad, R.M., 2017. Targeting acute myeloid leukemia stem cell signaling by natural products. Mol. Cancer 16, 13.
Taylor, W.F., Jabbarzadeh, E., 2017. The use of natural products to target cancer stem cells. Am. J. Cancer Res. 7, 1588–1605.
Torre, L.A., Siegel, R.L., Jemal, A., 2016. Lung cancer statistics. Adv. Exp. Med. Biol. 893, 1–19.
Tsai Ch, L.C., Cheng, Y.W., Lee, C.C., Liao, P.L., Lin, C.H., Huang, S.H., Kang, J.J., 2017. The inhibition of lung cancer cell migration by AhR-regulated autophagy. Sci. Rep. 7, e41927.
Wang, M., Hossain, M.S., Tan, W., Coolman, B., Zhou, J., Liu, S., Casey, P.J., 2010. Inhibition of isoprenylcysteine carboxylmethyltransferase induces autophagic-dependent apoptosis and impairs tumor growth. Oncogene 29, 4959–4970.
Wang, W.A., Groenendyk, J., Michalak, M., 2014. Endoplasmic reticulum stress associated responses in cancer. Biochim. Biophys. Acta 1843, 2143–2149.
Wong, V.K., Cheung, S.S., Li, T., Jiang, Z.H., Wang, J.R., Dong, H., Yi, X.Q., Zhou, H., Liu, L., 2010. Asian ginseng extract inhibits in vitro and in vivo growth of mouse lewis lung carcinoma via modulation of ERK-p53 and NF-kappaB signaling. J. Cell. Biochem. 111, 899–910.
Xi, G., Hu, X., Wu, B., Jiang, H., Young, C.Y., Pang, Y., Yuan, H., 2011. Autophagy inhibition promotes paclitaxel-induced apoptosis in cancer cells. Cancer Lett. 307, 141–148.
Yorimitsu, T., Nair, U., Yang, Z., Klionsky, D.J., 2006. Endoplasmic reticulum stress triggers autophagy. J. Biol. Chem. 281, 30299–30304.
Zhang, H.Y., Wang, Z.G., Lu, X.H., Kong, X.X., Wu, F.Z., Lin, L., Tan, X., Ye, L.B., Xiao, J., 2015. Endoplasmic reticulum stress: relevance and therapeutics in central nervous system diseases. Mol. Neurobiol. 51, 1343–1352.
Zhao, M., Wang, D.D., Che, Y., Wu, M.Q., Li, Q.R., Shao, C., Wang, Y., Cao, L.J., Wang, G.J., Hao, H.P., 2017. Ginsenosides synergize with mitomycin C in combating human non-small cell lung cancer by repressing Rad51-mediated DNA repair. Acta Pharmacol. Sin. 39, 449–458.